CSIRO PUBLISHING

International Journal of Wildland Fire **2008**, *17*, 500–514 www.publish.csiro.au/journals/ijwf

Evaluating the potential of Landsat TM/ETM+ imagery for assessing fire severity in Alaskan black spruce forests

Elizabeth E. Hoy[A,E], *Nancy H. F. French*[B], *Merritt R. Turetsky*[C], *Simon N. Trigg*[A,D] *and Eric S. Kasischke*[A]

[A]Department of Geography, University of Maryland, 2181 LeFrak Hall, College Park, MD 20742, USA.
[B]Michigan Tech Research Institute, Michigan Technological University, 3600 Green Court, Suite 100, Ann Arbor, MI 48105, USA.
[C]Department of Integrative Biology, University of Guelph, Guelph, ON, N1G 2W1, Canada.
[D]Department of Geographic Information Management, Cranfield University, Cranfield, Bedfordshire, UK.
[E]Corresponding author. Email: ehoy@umd.edu

Abstract. Satellite remotely sensed data of fire disturbance offers important information; however, current methods to study fire severity may need modifications for boreal regions. We assessed the potential of the differenced Normalized Burn Ratio (dNBR) and other spectroscopic indices and image transforms derived from Landsat TM/ETM+ data for mapping fire severity in Alaskan black spruce forests (*Picea mariana*) using ground measures of severity from 55 plots located in two fire events. The analysis yielded low correlations between the satellite and field measures of severity, with the highest correlation ($R^2_{\text{adjusted}} = 0.52$, $P < 0.0001$) between the dNBR and the composite burn index being lower than those found in similar studies in forests in the conterminous USA. Correlations improved using a ratio of two Landsat shortwave infrared bands (Band 7/Band 5). Overall, the satellite fire severity indices and transformations were more highly correlated with measures of canopy-layer fire severity than ground-layer fire severity. High levels of fire severity present in the fire events, deep organic soils, varied topography of the boreal region, and variations in solar elevation angle may account for the low correlations, and illustrate the challenges faced in developing approaches to map fire and burn severity in high northern latitude regions.

Additional keywords: composite burn index, *Picea mariana*, spectroscopic index.

Introduction

Forest fires are a major contributing factor to the world's carbon cycle. These fires release emissions into the atmosphere through the burning of the surface and canopy fuel matrix. Boreal forest regions can be considered both a source and sink for carbon because of their potential for forest fires and in providing avenues for reforestation. Increasing summer temperatures and changing atmospheric circulation patterns are influencing the fire regime in the boreal region (Gillett *et al*. 2004; Kasischke and Turetsky 2006; Skinner *et al*. 2006), although the overall effects of these changes on the landscape are still under study (Chapin *et al*. 2005). Remote sensing research has provided new approaches and methods to monitor landscape change as a result of fire.

Over the past decade, much research has focussed on using satellite remote sensing data to improve estimates of carbon emissions from fires in temperate and boreal forests. Satellite data products that provide information on the timing of fires and burned area are now routinely used to estimate emissions from fires in high northern latitude forests (Kasischke *et al*. 1995, 2005; Kajii *et al*. 2002; Soja *et al*. 2004; van der Werf *et al*. 2006; de Groot *et al*. 2007). While variations in biomass consumption have been shown to be a key uncertainty in estimating emissions (French *et al*. 2004), only a few studies carried out on individual fire events have used satellite remote sensing to map variations in severity (which is then used to estimate biomass consumption) (Michalek *et al*. 2000; Isaev *et al*. 2002; Campbell *et al*. 2007).

In terms of improving the accuracy of emissions from boreal regions, the deep organic soils found in the forests underlain by permafrost and the peatlands common to this region present particular challenges. Black spruce (*Picea mariana*) forests represent some 50% of the forest cover in Alaska and Canada (Kasischke and Johnstone 2005) and make up 60% of the area burned in Alaska and across Canada (Amiro *et al*. 2001). Fires in the deep surface organic layers of this forest type can release from 10 and up to 70 t C ha^{-1}; thus, variations in depth of burning represent a major source of uncertainty in estimating emissions from boreal fires (French *et al*. 2004; Kasischke *et al*. 2005).

The terms fire severity and burn severity are often used interchangeably in the fire science and remote sensing literature. We chose to interpret the terms fire severity and burn severity using the fire disturbance continuum described by Jain (2004) and discussed in detail by Lentile *et al*. (2006). Fire severity is considered to be the direct effects of the combustion process such as tree mortality and the losses of biomass in the forms of vegetation and soil organic material. Burn severity is a term used to describe the response of the environment to fire and is indicated

 10.1071/WF08107 1049-8001/08/040500

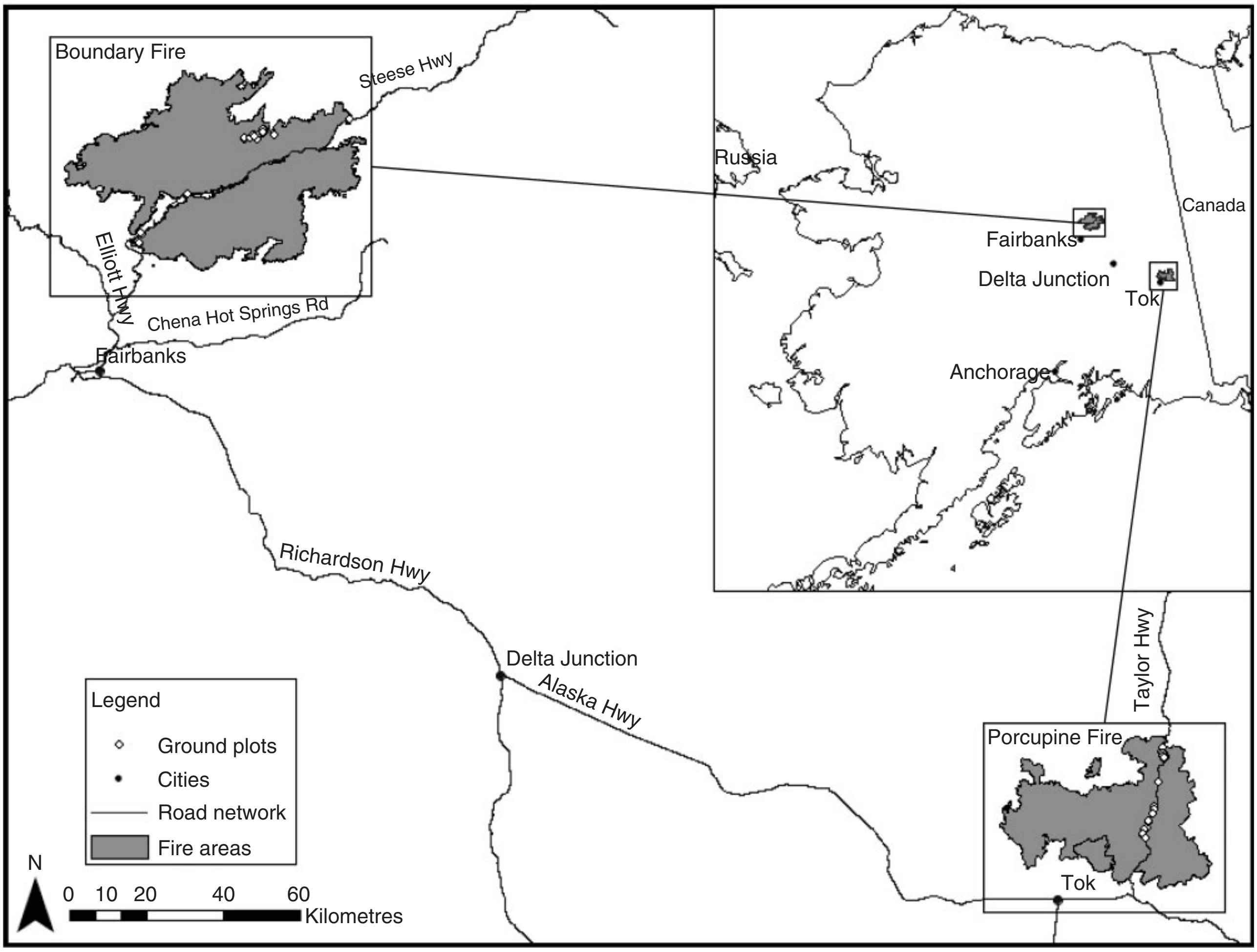

Fig. 1. Locations of the two 2004 Alaskan fires where the study sites were located. The study used field and Landsat data from 28 sites in the Boundary Fire and 27 sites in the Porcupine Fire.

through quantifying or predicting changes to the site as the result of damage from a fire. While burn severity is a function of fire severity, other site factors need to be considered (see French *et al*. 2008).

Numerous spectroscopic indices have been derived from satellite remote sensing data to quantify severity (French *et al*. 2008). The differenced Normalized Burn Ratio (dNBR) is a common method used to estimate severity based on the degree of change from pre-fire conditions as measured through the use of remote sensing data, and has often been correlated with a field estimate of severity called the composite burn index (CBI) (Key and Benson 2006). The CBI is used to estimate severity in situ for individual sites throughout the burned area. The relationship between the dNBR and CBI is then extrapolated over the entire burned area to produce a severity map. This severity mapping approach is currently used by the fire management community in the United States (Key and Benson 2006; Zhu *et al*. 2006). We have used this dNBR–CBI approach to determine the potential for using this index to analyse fire severity and to develop measures for assessing fuel consumption, not just burn severity.

Here we present the results of a study designed to test the sensitivity of different spectroscopic indices to different metrics of fire severity in interior Alaskan black spruce forests. The objectives of the study were to: (1) evaluate the potential of the dNBR–CBI approach to map fire severity in order to improve estimates of fuel consumption during fires and (2) evaluate and analyse the potential of the dNBR and other satellite indices to map other ground measures of fire severity (aside from CBI). We used sixteen single-date and seventeen two-date remotely sensed spectroscopic techniques designed for mapping land surface characteristics and vegetation change severity. This study was carried out by correlating the spectroscopic techniques with field measures of fire severity, including the CBI and other fire severity measures that can be used to estimate fuel consumption during fires.

Methods

Overview and study area

This study was carried out using remote sensing observations obtained from Landsat 5 and 7 (TM and ETM+) and field data from black spruce sites within two separate fire events that burned during the summer of 2004 in interior Alaska (Fig. 1; the Boundary Fire ($n = 28$ sites) and the Porcupine

Table 1. Landsat image information

Landsat image acquisition dates and sensor information for the two fire events used in this study. The geometric accuracy of the image registration is also presented

Fire event (date burned)	Data	Image date	Path/Row	Sensor	Geometric quality assessment (m)[A]	
					RMSE	s.d.
Boundary (late June 2004)	Pre-fire	18 July 2003	68/14	TM	12.02	11.41
	Post-fire	04 August 2004	69/14	ETM+	7.15	6.28
Porcupine (late June–late July 2004)	Pre-fire	10 September 2001	64/16	ETM+	23.89	23.67
	Post-fire	08 September 2004	66/15	TM	12.37	12.26

[A]The data for these columns come from the individual datasets for each image processed by the USGS EROS Data Center.

Fire ($n = 27$ sites)). Field data for this study were collected during the summers of 2005 and 2006. Data collected at each site included observations required to estimate the CBI, the depths of the remaining organic layer (which consisted of litter, lichen, mosses, char, and fibric, mesic and humic soil), measurements of the depth of the topmost adventitious root above mineral soil, and a visual estimate of the canopy fire severity. Fire severity characteristics derived from the field observations were then correlated with the spectroscopic metrics derived from the Landsat data.

Satellite data

The satellite data used in this study were obtained from the Landsat satellite series (Table 1). These data were initially processed for the inter-agency Burned Area Emergency Response Team (BAER) for the Alaska region by USGS EROS Data Center to Level 1 Terrain (L1T), meaning the data had been radiometrically corrected (to top of atmosphere reflectance values), geometrically corrected, and orthorectified (NASA Goddard Space Flight Center 2008). We then visually inspected the images and determined no further georegistration procedures were necessary because of the lack of an appreciable shift between images of the same location taken on different dates. From the geometric quality assessment data provided by the EROS Data Center for each image summarised in Table 1, it can be seen that three of the four images had an RMSE of <13 m while one image had an RMSE of 24 m. We did not use the thermal band in our analysis because of its lower spatial resolution.

We then examined each Landsat image for evidence of atmospheric contamination. At the time of data acquisition (late summer of 2004), some fires were still burning in the areas being imaged and smoke contamination was a concern. Fig. 2*a* depicts a Landsat bands 7, 4, 3 composite for the Porcupine Fire where some smoke is visible as a haze over the burned area. While the pre-fire images occurred on clear days, post-fire images on anniversary dates that were free of smoke and cloud cover were not always available. We assessed the level of atmospheric contamination based on top of atmosphere (TOA) reflectance measured in the visible bands (red, green and blue). These visible portions of the spectrum are highly sensitive to thick smoke and foggy conditions, making them useful for determining the level of atmospheric contamination. Sites affected by smoke in the two post-fire images were not used in the study – as a result, eight sites were excluded from the analysis from the Porcupine post-burn image. One Boundary Fire site was also excluded from the analysis because of a data gap caused by the scan line corrector being off in the Landsat 7 ETM+ post-fire image.

An image-to-image normalisation (dark object subtraction) was performed to reduce the effects of variations in atmospheric conditions between image pairs (e.g. pre- and post-fire). Average pixel values were extracted from three low-reflectance water bodies (large lakes) visible in both the pre-fire and post-fire images for each Landsat band used in this study (1–5 and 7). We assumed these values represented atmospheric scattering and we subtracted them from the respective bands to normalise each image (Chavez 1989). Bi-temporal image analysis should ideally use data acquired only one or two years apart and on anniversary dates to avoid noise in the analysis such as that from changing plant phenology and differing solar zenith angles throughout the year (Rogan *et al.* 2002; Epting *et al.* 2005). This type of analysis can be difficult in the boreal region and we used the best available data to perform a bi-temporal analysis (Table 1). Since we were interested in analysing the immediate impacts of fire we used post-burn Landsat images collected the same year as the fire and pre-fire imagery from one to three years before the fire. For example the images for the Porcupine Fire were ideal from the standpoint of anniversary dates as the images are only two days apart from one another (Table 1). Anniversary images were unavailable for the Boundary Fire; the best available match was two weeks apart (Table 1). One additional potential area of concern in using both Landsat 5 TM and Landsat 7 ETM+ data is that the regions of the wavelength spectrum for the different bands are slightly different. Previous studies, however, show that these differences do not cause significant errors in reflectances from areas with identical land cover (Huang *et al.* 2002).

Bilinear resampling (in which a weighted average is calculated for the four nearest pixels to a point) was used to extract the spectroscopic values for each site (Key and Benson 2006). This resampling technique is used to account for the geometric shift of approximately one-half of a pixel present within each image (Table 1). We then used the pre-processed Landsat TM/ETM+ data to generate the spectroscopic metrics including the Landsat spectroscopic bands, indices and transformations with potential for the remote estimation of fire and burn severity. Typical pre- and post-fire TOA reflectances from our study sites showed Band 4 decreased following fire while Band 7 increased following fire (Fig. 3). The differences in average Band 4 and Band 7 reflectance for the two sites were quite significant, most likely

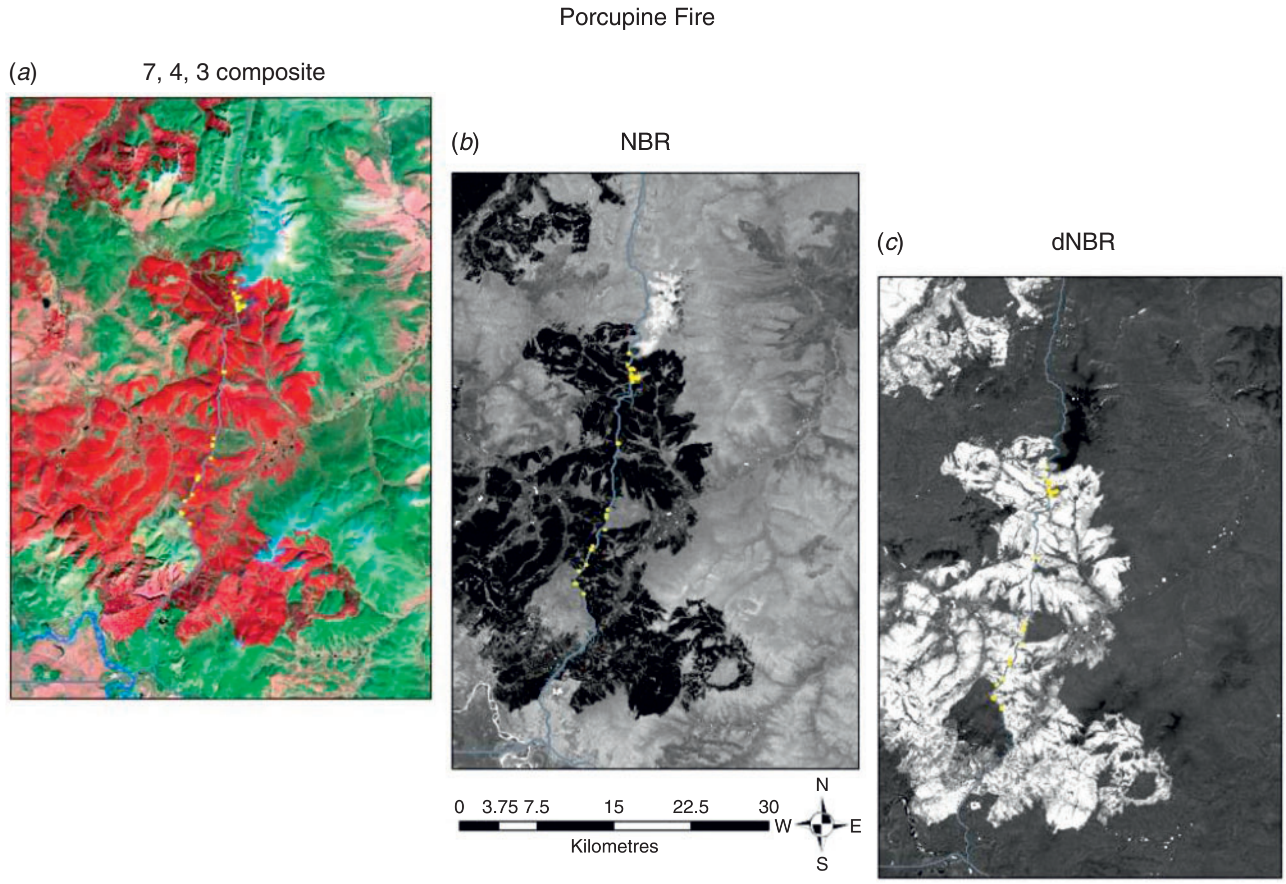

Fig. 2. Visualisation of the post-fire Porcupine Fire image first in a Landsat 7, 4, 3 bands composite (*a*), the post-NBR values (*b*) and finally the dNBR values (*c*). Our study plots can be seen along the Taylor Highway as yellow points. Smoke from the still burning fire can be seen in (*a*).

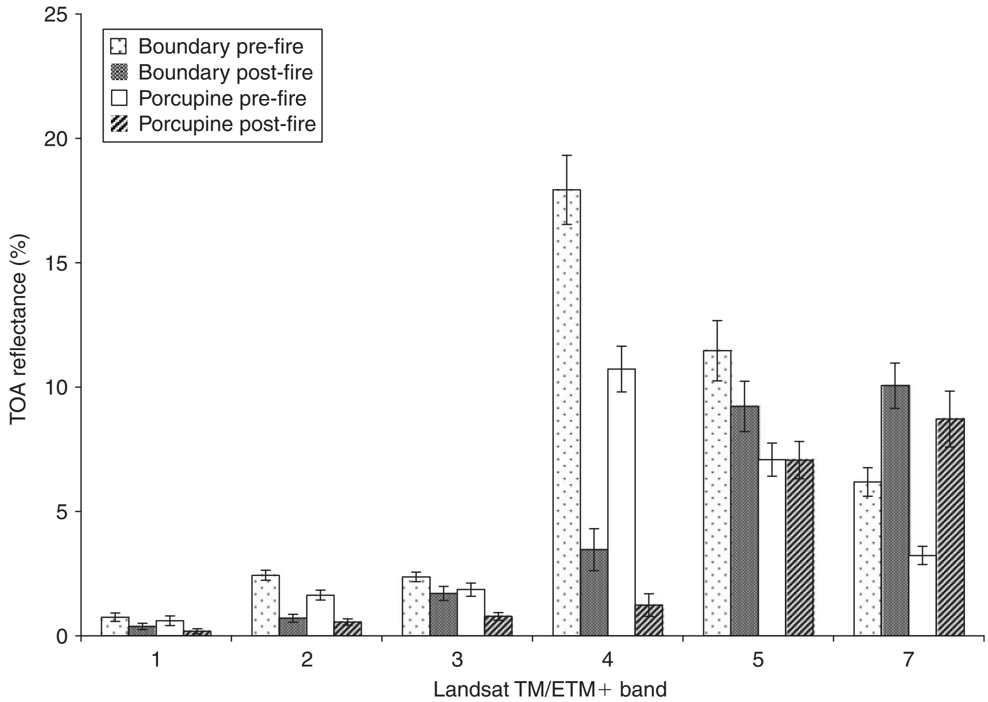

Fig. 3. The percentage of TOA reflectance and standard deviation of the six Landsat TM/ETM+ bands used in the study. For the reflectance measures: the Boundary Fire, $n = 28$; and for the Porcupine Fire, $n = 27$.

Table 2. Spectroscopic indices and transformations used in the study
Summary of spectroscopic indices and transformations derived from Landsat TM/ETM+ images used in this study. In this table, B stands for the Landsat TM/ETM+ band used to generate the index

Spectroscopic metric	Method of calculation
Band 4	Near-infrared band (0.76 to 0.90 μm)
Band 5	Shortwave-infrared band (1.55 to 1.70 μm)
Band 7	Shortwave-infrared band (2.08 to 2.35 μm)
NBR	$(B4 - B7)\ (B4 + B7)^{-1}$
dNBR	$NBR_{pre\text{-}fire} - NBR_{post\text{-}fire}$
RdNBR	$(NBR_{pre\text{-}fire} - NBR_{post\text{-}fire})(\sqrt{\lvert NBR_{pre\text{-}fire}\rvert})^{-1}$
Ratio 7/5	$(B7)\ (B5)^{-1}$
Ratio 7/4	$(B7)\ (B4)^{-1}$
Ratio 4/5	$(B4)\ (B5)^{-1}$
NDVI	$(B4 - B3)\ (B4 + B3)^{-1}$
SAVI	$(B4 - B3)\ (1 + L)\ (B4 + B3 + L)^{-1}$, where L = soil adjustment factor, 0.5
$MSAVI_2$	$0.5 \times (2 \times B4 + 1 - \sqrt{(2B4 + 1)^2 - 8 \times (B4 - B3)})$
TC1	Tasseled-cap brightness transformation $0.2043 \times B1 + 0.4158 \times B2 + 0.5524 \times B3 + 0.5741 \times B4 + 0.3124 \times B5 + 0.2303 \times B7$
TC2	Tasseled-cap greenness transformation $-0.1603 \times B1 - 0.2819 \times B2 - 0.4934 \times B3 + 0.7940 \times B4 + 0.0002 \times B5 - 0.1446 \times B7$
TC3	Tasseled-cap wetness transformation $0.0315 \times B1 + 0.2021 \times B2 + 0.3102 \times B3 + 0.1594 \times B4 - 0.6806 \times B5 - 0.6109 \times B7$
PCA1, PCA2, PCA3	Linear transforms based on correlation matrix of original Landsat bands 1, 2, 3, 4, 5 and 7

the result of differences in solar elevation between the times when the satellite imagery was collected for the two different fire events (Verbyla *et al.* 2008).

Spectroscopic indices and transforms

To assess mapping fire severity using both single-date and two-date approaches, we used spectroscopic indices and data transformations that have previously shown potential for detecting changes in surface reflectance as a result of disturbance (Table 2). In the single-date approach, a single post-fire Landsat image of the fire event was analysed. In the two-date approach, values from a post-fire Landsat image were subtracted from the corresponding pre-fire values. This procedure has been proposed to minimise differences between images as a result of factors other than disturbance from the fire (Key and Benson 2006).

The spectroscopic bands used in this study (Landsat TM/ETM+ bands 4, 5 and 7) are those previously shown to vary as a result of changes to live vegetation and soil characteristics following disturbance. NIR reflectance decreases following fire disturbance because of the loss of healthy green vegetation while the SWIR reflectance (especially Landsat band 7) increases due to several factors, which include the drying of vegetation and soil, decreased vegetation density, increased exposed substrate material, and the presence of charred fuels (Fig. 3) (Key and Benson 2006; Miller and Thode 2007). In addition to these three Landsat bands, simple ratios derived from these bands are also compared with the ground measures (Table 2). Simple ratios (Landsat 7/5, 7/4, and 4/5) were used as they have previously been shown to resolve problems of variable illumination due to rugged terrain (Ekstrand 1996).

We used two indices specifically developed for mapping burned areas and assessing fire and burn severity (Fig. 2). The Normalized Burn Ratio (NBR) is calculated from reflectance changes in the NIR (Landsat band 4 (B4) TM, 0.76–0.90 μm; ETM+, 0.78–0.90 μm) and SWIR (Landsat band 7 (B7) TM, 2.08–2.35 μm; ETM+, 2.09–2.35 μm) portions of the electromagnetic (EM) spectrum. The formula for the NBR when using Landsat imagery is $NBR = (B4 - B7)\ (B4 + B7)^{-1}$. The differenced NBR (dNBR) is calculated by subtracting the post-burn from the pre-burn NBR. A derivative to the dNBR, the relativised dNBR (RdNBR), was also used (Table 2). Miller and Thode (2007) developed this index to produce classifications of burn severity with less omission and commission errors for high severity fires.

The additional indices included the Normalized Difference Vegetation Index (NDVI), the soil adjusted vegetation index (SAVI), and the modified $SAVI_2$ ($MSAVI_2$) (Table 2). The SAVI was designed to account for soil brightness and calculated after Huete (1988). A value of 0.5 is used for the constant soil-brightness correction factor, L, as recommended for intermediate vegetation amounts (Huete 1988; Epting *et al.* 2005). The $MSAVI_2$, calculated as described in Qi *et al.* (1994), was used because it incorporates aspects of the SAVI but also has an increased dynamic range, which further decreases the noise due to soil brightness (Qi *et al.* 1994).

Fig. 4. Sample plot from the Boundary Fire. Plot photograph and measurements taken June 9, 2005. Overall CBI = 2.55, understorey CBI = 2.40, overstorey CBI = 3.00, post-NBR = −650 and dNBR = 1199. The NBR measurements have been multiplied by 1000. Photograph: E. S. Kasischke.

Two image transformations (the principal components analysis and the tasseled cap transformation) were selected based on their sensitivities to both soil and vegetation changes within Landsat TM/ETM+ imagery. A principal components analysis (PCA) was performed using a covariance matrix with band loadings. The tasseled cap (TC) transformations were calculated using the coefficients provided in Crist (1985). PCA transformations have been used to distinguish fire scars from non-burned areas as well as to discriminate dark soils and topographic shadowing from burned areas (Hudak and Brockett 2004). The TC transformation has been shown to be sensitive to changes in soil brightness and wetness as well as to changes in vegetation (Smith *et al*. 2005). Patterson and Yool (1998) found TC1 and PCA1 to be related (brightness), as well as TC2 and PCA2 (greenness). They did however find that TC3 and PCA3 (wetness components) were not strongly correlated. This discrepancy was believed to be due in part to the tendency of the PCA to be highly influenced by the dominant pixel values in the scene, in this case, unburned pixels (Patterson and Yool 1998). TC1 (brightness) was used based on its perceived sensitivity to high severity fires that burn the soil organic layer. In these situations, brightness may increase as mineral soil is exposed, which indicates a relatively complete combustion of the organic layer (Patterson and Yool 1998).

Field data

Initial reconnaissance of potential study sites that could be accessed from the road network was carried out in late May of 2005. During this reconnaissance, several burned black spruce forest sites were identified within the Boundary and Porcupine burns, with each containing a suitably large tract of forest (∼1 ha) that was relatively homogeneous in terms of tree diameter, density, and fire severity. It was important that the forest cover be relatively homogenous for an area of 8100 m^2, or the equivalent of the area of 3 × 3 Landsat pixels (nine pixels total), to ensure that the area of a single 30 × 30-m^2 Landsat pixel was captured within the measurement of a ground plot and to avoid bias within the sampling scheme (Key and Benson 2006). From these candidate sites, a sub-set was selected for sampling in order to cover the range of topographic positions and fire severities that existed within perimeters of the fires under study. The centre of each site was marked using a handheld GPS unit. General site conditions (slope, aspect and elevation of the site) were noted and four surface photographs were collected (Figs 4 and 5). Next, a 20 × 20-m^2 site for the collection of observations required to estimate the CBI (Key and Benson 2006) was established at the centre of the plot, and sampling transects were laid out for collection of the fire severity measures (Fig. 5).

Measuring the composite burn index

The composite burn index (CBI) was developed specifically to evaluate the dNBR and is used as a qualitative means to measure the magnitude of fire effects within individual forest stands (Key and Benson 2006). While the CBI has been commonly used to assess burn severity, it can be applied to fire severity

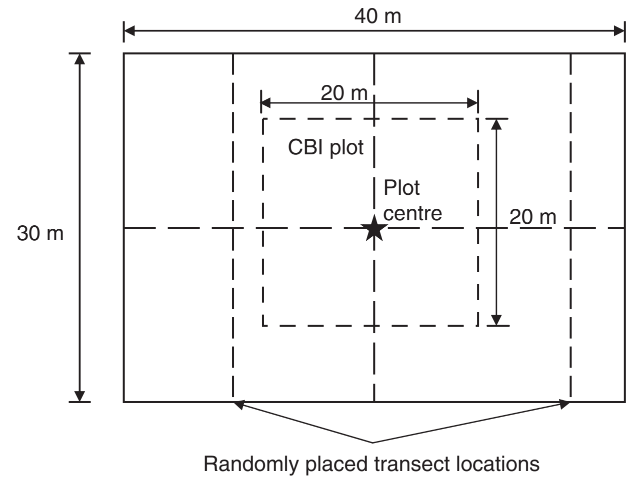

Fig. 5. Schematic of our study plot design. The plot centre is surrounded by a $20 \times 20\text{-m}^2$ square for the calculation of CBI. One 40-m and one 30-m transect were set up to bisect the plot. Two additional 30-m transects were then placed randomly along the 40-m transect and extending 15 m in each direction from the plot centre and perpendicular to the 30-m transect bisecting the plot.

with the understanding that it is the conditions left after the fire that are being analysed (Key and Benson 2006). With the exception of one site (when data were collected in the spring of 2006), data to estimate the CBI were collected during the summer of 2005, the year following the two fires. Data to calculate the CBI were collected from observations made within a $20 \times 20\text{-m}^2$ site using the data sheet developed by Key and Benson (2006). Data required to fill in the CBI form were obtained by visually examining five strata: (*a*) substrate; (*b*) herbs and low shrubs, and trees (>1 m); (*c*) tall shrubs and small trees (1 to 2 m); (*d*) intermediate trees (2 to 8 m); and (*e*) tall trees (>8 m) and rating damage on a scale of 0 to 3 for several characteristics within each stratum. There are three scores calculated for the CBI: the overall or average CBI (based on an average of all five components and here referred to as overall CBI), the understorey CBI (an average of components (*a*) through (*c*)) and the overstorey CBI (an average of components (*d*) and (*e*)).

For assessing severity in Alaska, the CBI form was modified based on discussions between representatives of the research and fire management communities in Alaska to account for the varied vegetation characteristics of the region (see Kasischke *et al*. 2008). Modifications were made to account for the presence of grass tussocks, moss, lichen, and the shorter shrub and tree heights found in this region. The grass tussock consumption measurement was added to the 'substrates' category of the CBI, while a measure of moss and lichen consumption was added to the 'herbs and low shrubs' category. The final modification to the CBI consisted of adjusting and defining the height requirements of the three tree categories of the CBI (tall shrubs and trees, intermediate trees, and big trees), as Alaskan black spruce trees only occasionally reach heights >8 m. The 'tall shrubs and trees' category was adjusted to include tree heights of only 1–2 m instead of trees from 1 to 5 m. The 'intermediate trees' were then defined as those of 2–8 m and 'big trees' as those >8 m.

Table 3. Canopy fire severity index

Criteria used to develop the canopy fire severity index. This index follows Kasischke *et al*. (2000) and can be used to assess the degree of burning that occurs only within the dominant tree species of the site, thus it is only a measure of the severity of crown fires. The index is based predominantly upon the percentage of crown foliage and branches consumed by fire and the survivorship or mortality of individual overstorey trees

Level	Criteria
0	No tree mortality
1	Tree deceased, no branches/foliage consumption
2	Needles and some small branches consumed
3	Some secondary branches remain
4	No secondary branches, >30% of primary branches remain
5	Less than 30% primary branches remain
6	No primary branches remaining, pole charring occurred

In many instances, comparing CBI estimates from observations made during the growing season following the fire with satellite data collected immediately following the fire would result in low correlations with dNBR because of changes to site attributes used to estimate CBI, especially shrub and tree mortality and invasion of colonising species. In the forests we used in our studies, the vegetation is highly flammable, and there is virtually no delayed mortality in these sites (Fig. 4). In our surveys of the burned sites in the 2004 fires, the level of invasion of colonizers we observed tended to be low except in sites with exposed mineral soils. For the most part, we visited sites with deep burning early in the 2005 growing season, when the growth of colonizers had not yet started. Thus, we believe the CBI collected during the growing season following the fire accurately depicted the conditions at the time the satellite data were collected.

Measuring crown and ground-layer fire severity

With respect to carbon cycling, measures of crown fire severity include the level of burning of biomass in the tree canopy, while measures of ground-layer fire severity include losses of biomass from the soil organic layer above the mineral soil. We felt that the criteria used to assess severity in the CBI method did not accurately reflect the biomass consumption that occurs during fires in black spruce forests, and additional approaches were used. We used the canopy fire severity index (CFSI) developed by Kasischke *et al*. (2000) to quantify the degree of burning of the crown foliage and branches (Table 3). For the surface organic layer, the fire severity measures included: (*a*) the average depth of the remaining surface organic layer; and (*b*) the absolute depth reduction in the surface organic layer and (*c*) the relative reduction in depth of the surface organic layer.

Ground and crown layer fire severity measurements were obtained by establishing a 40 m-long baseline oriented in a random direction through the centre of each site (Fig. 5). Three 30 m-long sample transects were then established that bisected the baseline at right angles: one at the site centre, and one on each side of the centre located at a random distance between 5 and 20 m along the baseline. Every overstorey tree >1 m in height within ±1 m of each transect was sampled by noting the level of consumption of foliage and branches based on a scale of 0 to 6 (the CFSI; Table 3). Every 5 m along each sample transect,

Table 4. Post-fire single-date correlations

Post-fire single-date adjusted R^2 values for correlations in the two study fires. The following significance levels are shown: ^{A}, $P \leq 0.0001$ (in bold); ^{B}, $P \leq 0.001$; ^{C}, $P \leq 0.05$. For the Boundary Fire, $n = 28$. Sample sites varied slightly across ground measures in the Porcupine Fire: CBI and canopy fire severity values are $n = 21$ and depth values are $n = 27$, while depth measurements were taken up to two years following the fire, CBI and CFSI were collected only one year following the fire, thus some sites have only partial datasets

Spectroscopic index	Overall CBI	CBI understorey	CBI overstorey	CFSI	Depth remaining
Boundary					
NBR	**0.59**^{A}	**0.55**^{A}	**0.42**^{A}	**0.53**^{A}	0.37^{B}
Band 4	0.39^{B}	0.37^{B}	0.24^{C}	0.38^{B}	0.29^{B}
Band 7	0.06	0.04	0.08	0.02	—
Ratio 7/5	**0.66**^{A}	**0.61**^{A}	**0.49**^{A}	**0.52**^{A}	**0.51**^{A}
Ratio 7/4	**0.49**^{A}	**0.47**^{A}	0.31^{C}	**0.43**^{A}	0.31^{C}
Ratio 4/5	**0.50**^{A}	**0.48**^{A}	0.32^{B}	**0.47**^{A}	0.26^{C}
NDVI	**0.53**^{A}	**0.52**^{A}	0.29^{C}	0.37^{B}	0.36^{B}
SAVI	**0.53**^{A}	**0.53**^{A}	0.30^{B}	0.38^{B}	0.36^{B}
$MSAVI_2$	**0.54**^{A}	**0.53**^{A}	0.29^{C}	0.38^{B}	0.36^{B}
TC2	**0.54**^{A}	**0.52**^{A}	0.34^{B}	**0.49**^{A}	0.40^{B}
PCA2	0.17^{C}	0.14^{C}	0.14^{C}	0.11^{C}	0.04
PCA3	—	—	0.04	—	—
Porcupine					
NBR	0.30^{C}	0.25^{C}	0.28^{C}	**0.83**^{A}	0.28^{C}
Band 4	0.27^{C}	0.21^{C}	0.28^{C}	**0.56**^{A}	0.14^{C}
Band 7	0.22^{C}	0.20^{C}	0.18^{C}	**0.59**^{A}	0.33^{C}
Ratio 7/5	0.42^{B}	0.40^{C}	0.24^{C}	**0.55**^{A}	0.33^{B}
Ratio 7/4	0.23^{C}	0.23^{C}	0.09	0.40^{C}	0.24^{C}
Ratio 4/5	0.20^{C}	0.16^{C}	0.21^{C}	**0.81**^{A}	0.26^{C}
NDVI	0.14	0.11	0.14	0.44^{B}	0.24^{C}
SAVI	0.15^{C}	0.12	0.15^{C}	0.46^{B}	0.24^{C}
$MSAVI_2$	0.15^{C}	0.13	0.13	0.37^{C}	0.22^{C}
TC2	0.33^{C}	0.27^{C}	0.35^{C}	**0.82**^{A}	0.31^{C}
PCA2	0.18^{C}	0.15^{C}	0.17^{C}	**0.62**^{A}	0.28^{C}
PCA3	0.29^{C}	0.25^{C}	0.26^{C}	**0.73**^{A}	0.38^{B}

a core of the remaining surface organic layer was extracted and the depths of the different layers (char, moss, lichen, and fibric, mesic and humic soil) were measured to within 0.5 cm. An organic layer core was also extracted and measured every 10 m along the baseline. In addition, the distance of the topmost adventitious root above mineral soil was measured on the nearest canopy tree above 2 m in height every 5 m along the sample transects. This distance was used to estimate the pre-fire depth of the surface organic layer (Kasischke *et al.* 2008). The measurements were then averaged to determine overall burn depths and consumption levels.

The depth of organic soil that remained was measured as the distance from the top of the remaining organic soil layer to the top of the A horizon. The absolute depth reduction is a measure of the difference between the pre-fire depth of the surface organic layer and the post-fire surface organic layer. When combined with the pre-fire organic layer depth, this measure can be used to estimate fuel consumption and carbon emissions. The relative depth reduction is the percentage of the depth burned during the fire compared with the pre-fire soil organic layer.

Analysis

We performed linear regression analysis using the least-squares approach within Microsoft Excel to correlate the spectroscopic indices (independent variables) and ground measures of burn severity (dependent variables) for both the single-date post-fire image approach and the two-date pre- and post-fire image approach. Here we present adjusted R^2 values and their level of statistical significance (P). This method was chosen to be consistent with prior comparisons of the dNBR and CBI approach (Epting *et al.* 2005; Key and Benson 2006). While this study followed the same general approach as Epting *et al.* (2005), additional fire severity measures (the CFSI and three depth reduction measurements) were compared with the spectroscopic indices.

Results and discussion

Although all satellite and field measures discussed in the methods section were compared (a total of 462 comparisons), only the most significant results are presented (Tables 4 and 5; Figs 6 and 7). Our discussions centre around three categories of field measurement of burn severity: the CBI, CSFI, and remaining organic layer depth. Because of the overall low level of correlation, the comparisons between the satellite indices and relative and absolute depth reduction are not presented.

CBI correlations

One of the most striking trends in our results was that the correlations between CBI and the various indices derived from Landsat

Table 5. Two-date correlations

Two-date image adjusted R^2 values for correlations in the two study fires. The following significance levels are shown: ^{A}, $P \le 0.0001$ (in bold); ^{B}, $P \le 0.001$; ^{C}, $P \le 0.05$. For the Boundary Fire, $n = 28$. Sample sites varied slightly across ground measures in the Porcupine Fire: CBI and canopy fire severity values are $n = 21$ and depth values are $n = 27$, while depth measurements were taken up to 2 years following the fire, CBI and canopy were collected only one year following the fire, thus some sites have only partial datasets

Spectroscopic index	Overall CBI	CBI understorey	CBI overstorey	CFSI	Depth remaining
Boundary					
dNBR	**0.52**^{A}	**0.48**^{A}	0.37^B	**0.48**^{A}	**0.46**^{A}
RdNBR	**0.58**^{A}	**0.54**^{A}	**0.43**^{A}	**0.53**^{A}	0.37^B
Band 4	0.01	—	0.05	—	0.26^C
Band 7	0.26^C	0.24^C	0.21^C	0.26^C	0.12^C
Ratio 7/5	**0.55**^{A}	**0.51**^{A}	**0.42**^{A}	**0.43**^{A}	**0.58**^{A}
Ratio 7/4	**0.49**^{A}	**0.47**^{A}	0.30^C	**0.43**^{A}	0.32^B
Ratio 4/5	—	—	—	—	0.02
NDVI	**0.45**^{A}	**0.43**^{A}	0.29^C	0.36^B	**0.42**^{A}
SAVI	**0.46**^{A}	**0.44**^{A}	0.29^C	0.36^B	**0.43**^{A}
$MSAVI_2$	**0.51**^{A}	**0.49**^{A}	0.30^C	0.38^B	0.40^B
TC2	0.02	—	0.06	—	0.29^C
PCA2	0.18^C	0.16^C	0.17^C	0.15^C	0.29^C
PCA3	0.11^C	0.09	0.10	0.11^C	—
Porcupine					
dNBR	0.34^C	0.29^C	0.31^C	**0.82**^{A}	0.29^C
RdNBR	0.30^C	0.25^C	0.28^C	**0.80**^{A}	0.26^C
Band 4	0.18^C	0.19^C	0.06	**0.64**^{A}	0.20^C
Band 7	0.29^C	0.23^C	0.28^C	**0.57**^{A}	0.35^B
Ratio 7/5	0.45^B	0.41^B	0.31^C	**0.61**^{A}	0.29^C
Ratio 7/4	0.23^C	0.23^C	0.09	0.41^C	0.25^C
Ratio 4/5	—	—	0.02	—	—
NDVI	0.15^C	0.12	0.16^C	0.42^B	0.22^C
SAVI	0.16^C	0.12	0.17^C	0.44^B	0.22^C
$MSAVI_2$	0.16^C	0.13	0.14	0.36^B	0.21^C
TC2	0.20^C	0.19^C	0.12	**0.67**^{A}	0.22^C
PCA2	0.10	0.05	0.18^C	0.06	0.21^C
PCA3	0.29^C	0.26^C	0.21^C	**0.65**^{A}	0.39^B

data were much higher for the Boundary Fire sites than for the Porcupine Fire sites, for both the single-date (Table 4; Fig. 6) and two-date (Table 5; Fig. 7) datasets. There were no significant differences in the stand characteristics and levels of fire severity as measured by the various field methods between the sites in the two fire events. This leads us to believe that the sources for the differences in the levels of correlations were in the NBR and dNBR values estimated from the Landsat TM/ETM+ data collected over these two sites (Table 6). Possible sources of variation in the satellite indices are discussed later in this section.

Both Epting *et al.* (2005) and Allen and Sorbel (2008) carried out correlations between CBI and NBR/dNBR based on data collected in burned black spruce forests in Alaska. Epting *et al.* (2005) showed that the NBR resulted in higher correlations with the overall CBI than did dNBR for both open and closed canopy spruce forests in Alaska. Our results showed that overall CBI had a higher correlation with NBR for the Boundary Fire sites, but that dNBR had the higher correlation with the overall CBI from the Porcupine sites. The range in correlations of the overall CBI and dNBR found by Epting *et al.* (2005) ($R^2 = 0.14$ to 0.28) were lower than the levels found by our analyses ($R^2_{\text{adjusted}} = 0.34$ to 0.52), whereas the correlations between CBI and NBR were higher in Epting *et al.* ($R^2 = 0.36$ to 0.66) than in our study ($R^2_{\text{adjusted}} = 0.30$ to 0.59). The results from our study were lower than the correlations of $R^2 = 0.72$ found by Allen and Sorbel (2008). Correlations between both dNBR and NBR and CBI were higher for the overall CBI than they were for the two components of CBI (understorey and overstorey), which is consistent with the findings of Allen and Sorbel (2008). While the RdNBR resulted in higher correlations with the CBI values than the dNBR for the Boundary Fire sites, it resulted in lower correlations in the Porcupine Fire sites.

The scatter plots of CBI as a function of NBR, dNBR, and RdNBR in Figs 6 and 7 show that there are differences in the slopes of the regression lines between the data from the Boundary and Porcupine Fires. Holden *et al.* (2007) used dNBR data collected over a 24-year period to study trends in burn severity. This study was based on the assumption that the regression relationship developed between dNBR and CBI from one set of data could be applied across data collected in different years. When we used the regression equation developed from the Boundary Fire dNBR and overall CBI data ($y = 0.0012x + 1.25$) to predict the overall CBI for the Porcupine Fire sites, the correlation between the observed and predicted values was

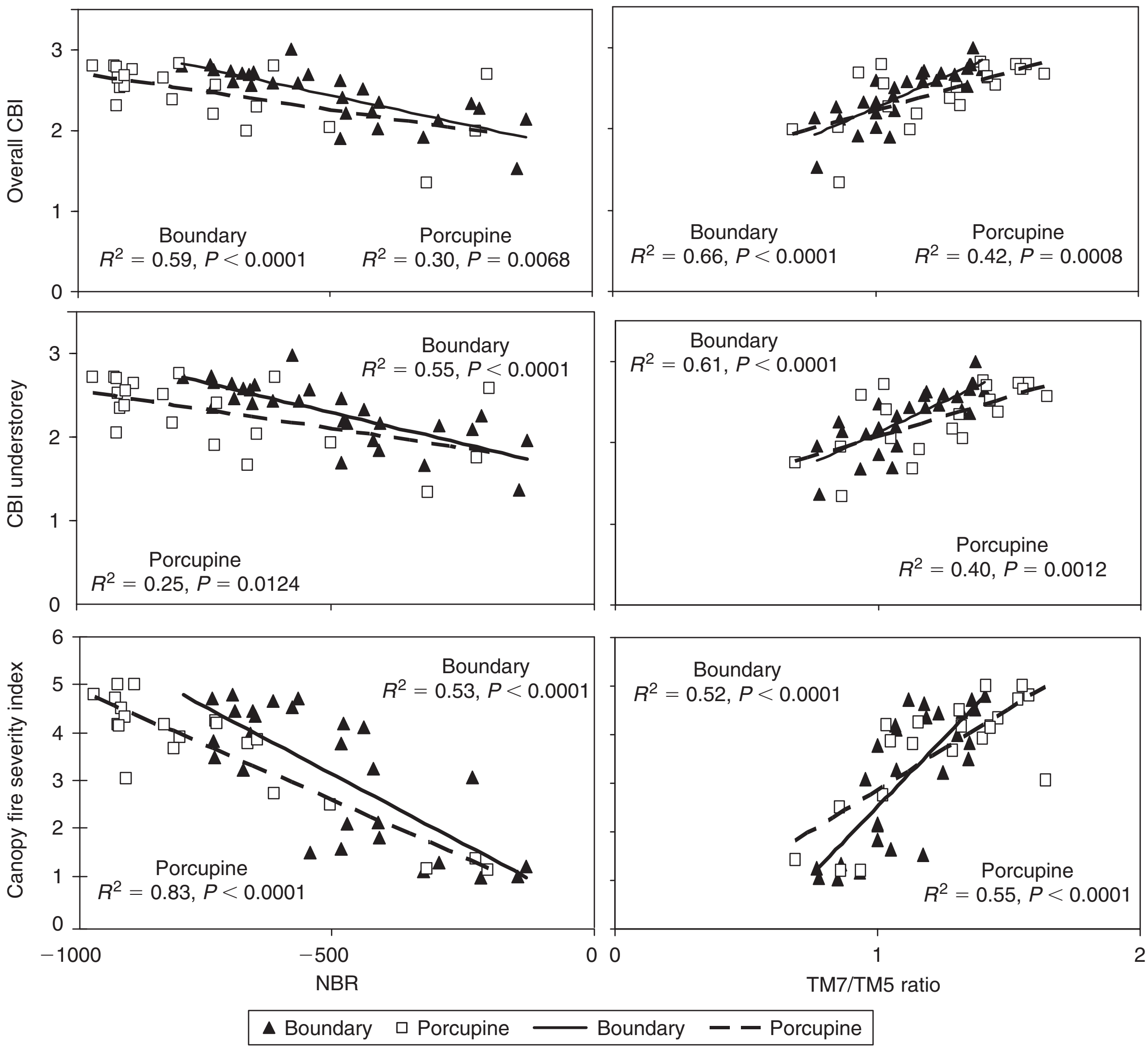

Fig. 6. Single-date comparison of the NBR and 7/5 ratio indices *v.* three different ground measures of fire severity for data from the Boundary and Porcupine Fires. These plots represent those indices that showed the greatest potential to estimate fire severity.

low ($R^2_{\text{adjusted}} = 0.34$, $P = 0.003$), and the slope of the regression line indicated that the CBI was under-predicted by 30% because of the higher dNBR values obtained for the sites in the Porcupine Fires (Fig. 8). When the reverse analysis was performed using the regression equation from the Porcupine Fire ($y = 0.0008x + 1.39$) to predict the Boundary Fire overall CBI values, a correlation of $R^2_{\text{adjusted}} = 0.52$, $P < 0.0001$ was found, however the slope of the regression line indicated that the CBI was over-predicted by almost 50% (Fig. 8).

Correlations between the other satellite remote sensing indices and CBI followed the same general trend found with NBR and its derivatives. Overall, the correlations were higher using data from the Boundary Fire sites than with data from the Porcupine Fire sites, and the correlations were higher using the overall CBI than its components (overstorey and understorey) (Tables 4 and 5). Of all the satellite indices evaluated for this study, the ratio of Landsat bands 7/5 (7/5 ratio) resulted in the highest correlations with CBI for the single-date analysis (Tables 4 and 5, Figs 6 and 7). Our results were consistent with the findings of Epting *et al*. (2005), who found that the 7/5 ratio had higher correlations with CBI than NBR or dNBR at some of the sites they studied. On average, Epting found that the highest correlations existed between CBI and NBR for both single- and two-date data, while the second best correlation was found between CBI and the 7/5 ratio for single-date data, and with the 7/4 ratio for two-date data. In our two-date analysis, the Boundary Fire RdNBR was the most strongly correlated with the CBI, while in the Porcupine Fire it was again the 7/5 ratio.

In summary, the results from our studies in Alaskan black spruce forests show that the relationship between CBI and NBR and its derivatives (dNBR and RdNBR) and other satellite indices is highly variable across sites that were collected in different years and between different sites that burned during different times of the same year. This finding reinforces a conclusion of

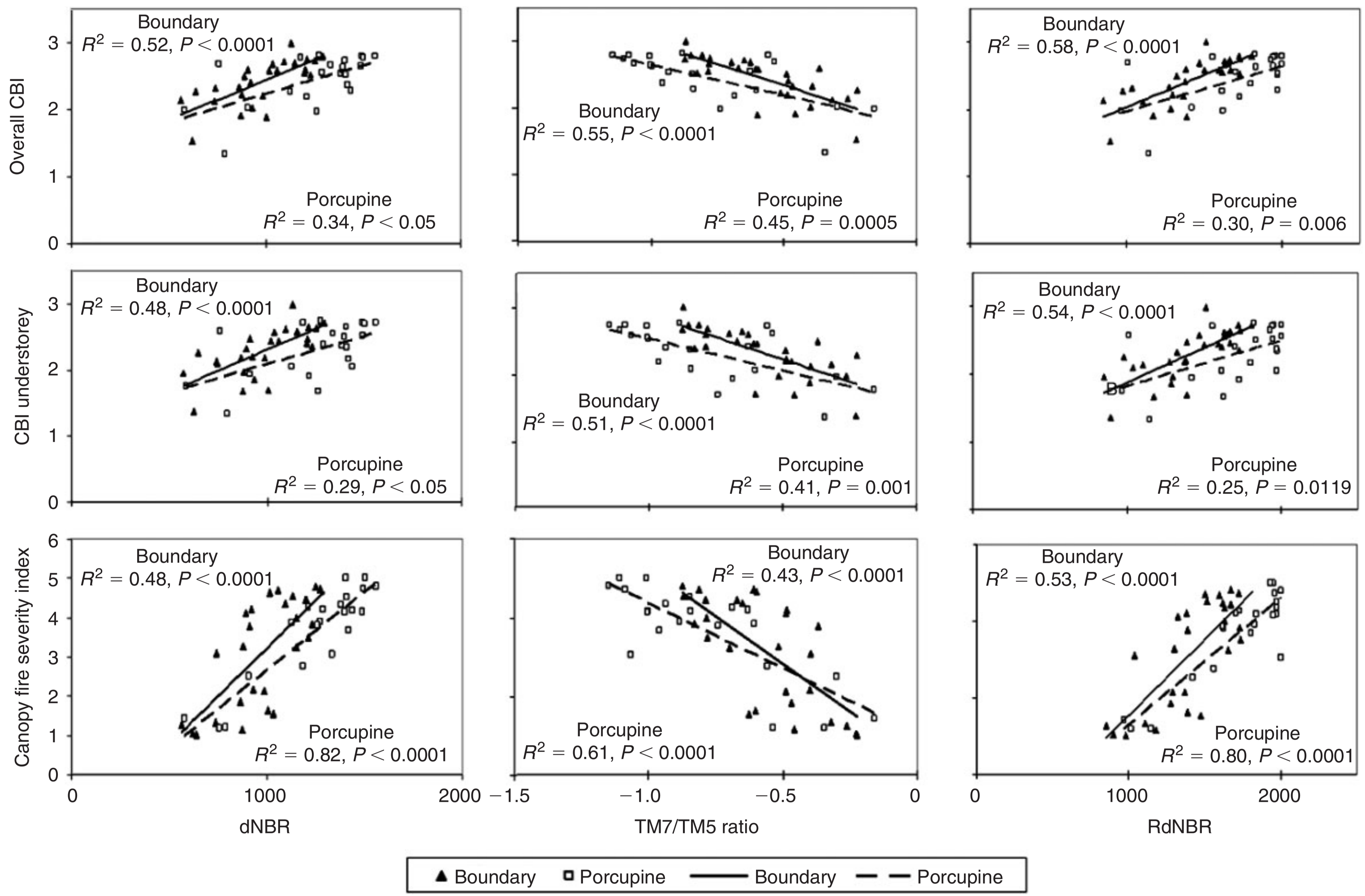

Fig. 7. Two-date comparison of the dNBR, differenced 7/5 ratio, and RdNBR indices *v.* three different ground measures of fire severity for data from the Boundary and Porcupine Fires. These plots represent those indices that showed the greatest potential to estimate fire severity.

Table 6. NBR, dNBR and CBI scores for each fire

Average NBR, dNBR and CBI scores for each fire and associated standard deviations (s.d.). The NBR measurements have been multiplied by 1000. For the NBR measures: the Boundary Fire, $n = 28$; and for the Porcupine Fire, $n = 27$. For the CBI values: the Boundary Fire, $n = 28$; and for the Porcupine Fire, $n = 21$

Fire event	Measure	Pre-fire NBR	Post-fire NBR	dNBR	Overall CBI	Understorey CBI	Overstorey CBI
Boundary	Mean value	488.08	−504.29	992.37	2.43	2.31	2.81
	s.d.	43.24	183.46	203.48	0.34	0.37	0.32
	Coefficent of variance	8.86	36.38	20.50	13.82	16.04	11.27
Porcupine	Mean value	535.60	−728.99	1264.59	2.45	2.31	2.86
	s.d.	77.32	225.70	272.33	0.38	0.41	0.39
	Coefficent of variance	14.44	30.96	21.54	15.45	17.64	13.61

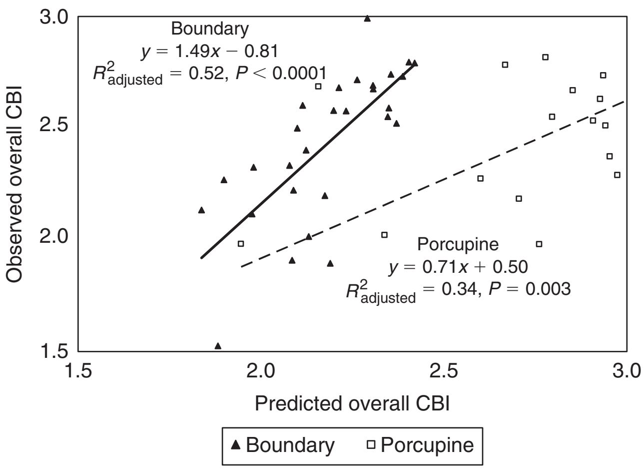

Fig. 8. Plot of observed overall CBI values as a function of the predicted overall CBI based on linear regression equations developed from data from each of the fire events. An equation from the Boundary Fire was used to predict the Porcupine Fire CBI values and vice versa.

Roy *et al*. (2006) in that the relationship of the dNBR to fire or burn severity was found to be inconsistent across burned areas and ecosystem types.

CFSI correlations

For all the remote sensing indices used in our study, the correlations with the CFSI were consistently higher than with the CBI overstorey data. In particular, the CFSI data from the Porcupine Fire sites had a much higher level of correlation with the remote sensing indices than the CBI overstorey data, and the CFSI data from the Porcupine Fire sites had much higher correlations than the data from the Boundary Fire sites (Tables 4 and 5).

There are several explanations for these differences. First, the criteria used to estimate the overstorey CBI values are based on evaluation of percent tree mortality, percent of tree trunks that are browned, percent of tree trunks that are scorched, and scorch height. Because most of the burned area in black spruce forests occurs in crown fires, the levels of these factors are always high, which results in very little variation in the CBI overstorey values (data from the two fire events show a mean of 2.83, s.d. = 0.35) (Fig. 9). The CFSI measured levels of consumption of crown fuels in the black spruce forests, which was more variable across our sites (mean = 3.39, s.d. = 1.30) (Fig. 9). Our results clearly show that the CFSI explained more of the variation in the satellite spectroscopic indices than did the CBI overstorey.

Second, the higher correlations between the satellite indices and the CFSI values from the Porcupine sites and Boundary sites can be explained by consideration of the variations in the solar elevation angle. The Landsat data used for the Porcupine site were collected in early September, while the data for the Boundary sites was collected in early August (Table 1). Because the solar elevation angle is lower in September than in August, the degree of shadowing would be greater in the Porcupine Fire sites than in the Boundary Fire sites at the time of Landsat data collections. Previous studies have shown that variations in tree structure can be inferred through the analysis of Landsat TM data because of the influence of tree shadowing on the spectroscopic reflectances (Cohen and Spies 1992). The impacts of variations in canopy consumption on tree shadows may explain the higher correlations observed in the Porcupine Fire data with CFSI.

Depth of remaining organic layer correlations

The correlations between the satellite indices and the measures related to consumption of the surface organic layer were low overall. There were no significant correlations between the satellite indices and the absolute and relative depth reduction, while the correlations with depth remaining were generally low, and lower than those found for CBI understorey for the Boundary Fire sites and higher than those found for the Porcupine Fire sites (Tables 4 and 5). The highest correlations were found with the 7/5 ratio ($R^2_{adjusted} = 0.51$ for the single-date data and $R^2_{adjusted} = 0.58$ for the two-date data).

Sources of uncertainties

The low level of correlations found in our study between satellite indices and surface measures of fire severity, and the differences in correlation between data collected in two separate fire events led us to consider possible reasons for these results. Four areas were identified.

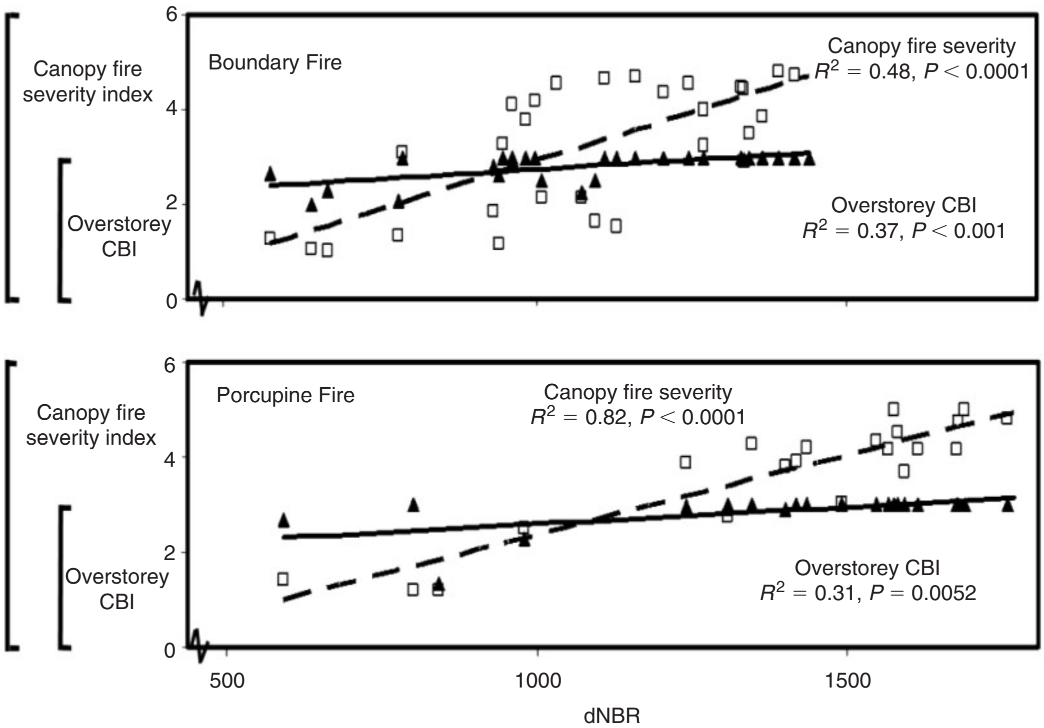

Fig. 9. Comparisons between the CFSI and the overstorey CBI measure for both fires. The overstorey CBI appears to saturate at the high end of its range (0 to 3) when compared with the CFSI range (0 to 6).

The first reason has to do with the ability of the CBI to capture the variability in damage from fires that occur in black spruce forests. For the canopy layer, this shortcoming is clearly illustrated in our analyses of the correlations between the satellite indices and the CFSI (Fig. 9). Measures of the other CBI strata showed that they had narrow ranges as well (Table 6), which indicates that variations in surface characteristics related to fire severity in black spruce forests are not well captured by the CBI approach. While the understorey CBI showed promise in one fire event, the correlations between the satellite indices with other surface measures of fire severity were also low.

Second, a recent study by Verbyla *et al.* (2008) highlights the dramatic changes that occur within the solar elevation angles in Alaska over the course of the growing season, which strongly influence spectroscopic reflection through controls on atmospheric attenuation and the scattering of EM radiation. This can then affect bidirectional reflectance from the surface, and influence the degree of vegetation shadowing. Verbyla *et al.* (2008) show that variations in solar elevation angle result in changes in the NBR from the same unburned stands over the growing season, which means that for the same level of fire severity, one would derive a different dNBR depending on the date the Landsat data were obtained. Thus, approaches to correct Landsat reflectance values need to be developed and applied to the data to correct for these effects. In addition, variations in solar elevation angle and site slope will influence vegetation shadowing. Therefore, studies need to be carried out to assess the influence of shadowing on surface reflectance.

Third, variations in the local angle of incidence of the solar radiation with respect to the ground surface affect bidirectional scattering of solar radiation. Thus topographic variation between sites is likely to result in differences in the reflectance values recorded in the Landsat TM/ETM+ bands. This influence results in differences for the correlation between CBI and the spectroscopic indices as a function of slope and aspect for the sites from both the Porcupine and Boundary Fires (Table 7). While topographic normalisation techniques do exist (Colby 1991; Ekstrand 1996; Gu and Gillespie 1998), their effectiveness needs to be evaluated in this region.

Table 7. Topographical influences to the dNBR

Correlations between CBI and dNBR as a function of slope and aspect for sites located in the Boundary and Porcupine Fires. The following significance levels are shown: A, $P \leq 0.0001$ (in bold); B, $P \leq 0.001$; C, $P \leq 0.05$

Topography	Boundary		Porcupine	
	$R^2_{adjusted}$	n	$R^2_{adjusted}$	n
North slope	0.65	5	0.57^C	7
South slope	0.26	11	0.38^C	11
East and west	0.69^B	12	0.02	3
Slope >2%	**0.57^A**	22	0.36^C	15

Finally, studies in other forest and vegetation types indicate that the relationship between dNBR and CBI becomes non-linear at high levels of fire severity (van Wagtendonk *et al.* 2004). It could very well be that such non-linearities exist for black spruce forests, which could lead to low correlations when the majority of fires are high severity events.

Conclusions and recommendations

The primary finding of our study was that the NBR and its derivatives, as well as the other spectroscopic indices and image transforms derived from satellite imagery, were not suitable for the mapping of fire severity in black spruce forests, and thus cannot be used to estimate carbon consumed during fires. While there appears to be some potential for mapping of canopy fire severity using late-growing season satellite imagery, the low correlations between the satellite indices and measures of depth of burning in the surface organic layer indicate that using traditional approaches of correlating spectroscopic reflectance data with field observations has little potential for estimating surface fuel consumption. This finding is consistent with previous research that found little correlation between dNBR and surface measures of fire severity (Kokaly *et al*. 2007).

The CBI approach has limitations in quantifying damage that occurs from fires in black spruce forests, and alternate approaches need to be developed to study surface characteristics that are responsible for variations in surface reflectance in these sites. In particular, field-based spectroscopic reflectance measurements should be collected to understand what scene characteristics are contributing to the satellite signatures (Trigg and Flasse 2001; Smith *et al*. 2005). Such studies would provide the basis for identifying the scene and severity characteristics that result in variations in the satellite signature. In addition, since changes in solar and local angles of incidence also introduce considerable variation in the satellite spectroscopic signatures, more rigorous approaches to account for these factors need to be investigated. For example, Ekstrand (1996) has shown that rugged terrain can strongly influence the response related to incident angle for Landsat TM bands 4 and 5, and to a lesser extent bands 2, 3, and 7. This study showed that incorporating a terrain correction function made distinguishing higher degrees of tree defoliation possible (Ekstrand 1996).

Understanding fire severity and the affects of the changing fire regime on the global carbon cycle is important to create meaningful policies and environmental guidelines. The Canadian boreal forests are specifically mentioned in the Kyoto protocol because of their potential as a carbon sink (Amiro *et al*. 2001). The dNBR was originally developed to analyse burned areas and this index could potentially be paired with other quantitative measures of fire severity to derive useful information that concerns fire severity and carbon emissions. Using the dNBR index in combination with forest cover maps derived from Landsat data could result in improved accuracy in distinguishing unburned islands from burned areas, a variable that can decrease burned area estimates by 3–5% (Amiro *et al*. 2001). A hybrid approach in which the dNBR is used for mapping burned area and other satellite-based approaches are used for fire severity estimates may provide better estimates in the boreal area and other areas of extreme solar angles and topographic positions.

Our results show that there is a need for the fire science community to go beyond testing the potential of different spectroscopic indices using R^2 values from regression models, and move towards independently validating methods using data from test sites other than those used to initially develop the algorithms. In particular, there are significant variations in solar elevation angles during the growing (fire) season at all latitudes. Since variations in solar elevation angle influence atmospheric affects, scene shadowing, and bidirectional reflectance, one would expect variable spectroscopic reflectances from burns with similar levels of fire severity that occur at different time periods. Until more independent validation of the dNBR–CBI approach occurs, caution should be used in interpreting results of long-term variations in fire severity using this method.

Acknowledgements

The research in the paper was supported by NASA through Grant NNG04GD25G and the Bonanza Creek Long-Term Ecological Research program (USFS grant number PNW01-JV11261952–231 and NSF grant number DEB-0080609). We thank Evan Ellicott, Evan Kane, Gordon Shetler, Luz Silverio, Sam Upton, Richard Powell and Lucas Spaete for assisting in the collection of field data. We also thank the two anonymous reviewers who provided us with such valuable insight and direction.

References

Allen JL, Sorbel B (2008) Assessing the differenced Normalized Burn Ratio's ability to map burn severity in the boreal forest and tundra ecosystems of Alaska's national parks. *International Journal of Wildland Fire* **17**, 463–475. doi:10.1071/WF08034

Amiro BD, Todd JB, Wotton BM, Logan KA, Flannigan MD, Stocks BJ, Mason JA, Martell DL, Hirsch KG (2001) Direct carbon emissions from Canadian forest fires, 1959–1999. *Canadian Journal of Forest Research* **31**, 512–525. doi:10.1139/CJFR-31-3-512

Campbell J, Donato D, Azuma D, Law B (2007) Pyrogenic carbon emissions from a large wildfire in Oregon, United States. *Journal of Geophysical Research* **112**, G04014. doi:10.1029/2007JG000451

Chapin FS, III, Sturm M, Serreze MC, McFadden JP, Key JR, Lloyd AH, McGuire AD, Rupp TS, Lynch AH, Schimel JP, Beringer J, Chapman WL, Epstein HE, Euskirchen ES, Hinzman LD, Jia G, Ping CL, Tape KD, Thompson CDC, Walker DA, Welker JM (2005) Role of land-surface changes in Arctic summer warming. *Science* **310**, 657–660. doi:10.1126/SCIENCE.1117368

Chavez PS, Jr (1989) Radiometric Calibration of Landsat Thematic Mapper Multispectral Images. *Photogrammetric Engineering and Remote Sensing* **55**, 1285–1294.

Cohen WB, Spies TA (1992) Estimating structural attributes of Douglas-Fir/Western Hemlock forest stands from Landsat and SPOT imagery. *Remote Sensing of Environment* **41**, 1–17. doi:10.1016/0034-4257(92)90056-P

Colby JD (1991) Topographic normalization in rugged terrain. *Photogrammetric Engineering and Remote Sensing* **57**, 531–537.

Crist EP (1985) A TM tasseled cap equivalent transformation for reflectance factor data. *Remote Sensing of Environment* **17**, 301–306. doi:10.1016/0034-4257(85)90102-6

De Groot W, Landry R, Kurz W, Anderson K, Englefield P, Fraser RH, Hall RJ, Banfield E, Raymond D, Decker V, Lynham T, Pritchard J (2007) Estimating direct carbon emissions from Canadian wildland fires. *International Journal of Wildland Fire* **16**, 593–606. doi:10.1071/WF06150

Ekstrand S (1996) Landsat-TM based forest damage assessment: correction for topographic effects. *Photogrammetric Engineering and Remote Sensing* **62**, 151–161.

Epting J, Verbyla D, Sorbel B (2005) Evaluation of remotely sensed indices for assessing burn severity in interior Alaska using Landsat TM and ETM+. *Remote Sensing of Environment* **96**, 328–339. doi:10.1016/J.RSE.2005.03.002

French NHF, Goovaerts P, Kasischke ES (2004) Uncertainty in estimating carbon emissions from boreal forest fires. *Journal of Geophysical Research* **109**, D14S08. doi:10.1029/2003JD003635

French NHF, Allen JL, Hall RH, Hoy EE, Kasischke ES, Murphy KA, Verbyla DL (2008) Using landsat data to assess fire and burn severity in the North American boreal forest region: an overview and summary of results. *International Journal of Wildland Fire* **17**, 443–462. doi:10.1071/WF08007

Gillett NP, Weaver AJ, Zwiers FW, Flannigan MD (2004) Detecting the effect of climate change on Canadian forest fires. *Geophysical Research Letters* **31**, L18211. doi:10.1029/2004GL020876

Gu D, Gillespie A (1998) Topographic normalization of Landsat TM images of forest based on subpixel sun–canopy–sensor geometry. *Remote Sensing of Environment* **64**, 166–175. doi:10.1016/S0034-4257(97)00177-6

Holden ZA, Morgan P, Crimmins M, Steinhorst R, Smith AMS (2007) Fire season precipitation variability influences fire extent and severity in a large southwestern wilderness area, United States. *Geophysical Research Letters* **34**, L16708. doi:10.1029/2007GL030804

Huang C, Wylie B, Yang L, Homer C, Zylstra G (2002) Derivation of a tasselled cap transformation based on Landsat 7 at-satellite reflectance. *International Journal of Remote Sensing* **23**, 1741–1748. doi:10.1080/01431160110106113

Hudak AT, Brockett BH (2004) Mapping fire scars in a southern African savannah using Landsat imagery. *International Journal of Remote Sensing* **25**, 3231–3243. doi:10.1080/01431160310001632666

Huete AR (1988) A Soil-Adjusted Vegetation Index (SAVI). *Remote Sensing of Environment* **25**, 295–309. doi:10.1016/0034-4257(88)90106-X

Isaev AS, Korovin GN, Bartalev SA, Ershov DV, Janetos A, Kasischke ES, Shugart HH, French NH, Orlick BE, Murphy TL (2002) Using remote sensing to assess Russian forest fire carbon emissions. *Climatic Change* **55**, 235–249. doi:10.1023/A:1020221123884

Jain TB (2004) Tongue-tied: confused meanings for common fire terminology can lead to fuels mismanagement. *Wildfire* **June/July**, 22–26.

Kajii Y, Kato S, Streets D, Tsai N, Shvidenko A, Nilsson S, McCallum I, Minko N, Abushenko N, Altyntsev D, Khodzer T (2002) Boreal forest fires in Siberia in 1998: estimation of area burned and emissions of pollutants by advanced very high resolution radiometer data. *Journal of Geophysical Research* **107**, 4745. doi:10.1029/2001JD001078

Kasischke ES, Johnstone JF (2005) Variation in postfire organic layer thickness in a black spruce forest complex in interior Alaska and its effects on soil temperature and moisture. *Canadian Journal of Forest Research* **35**, 2164–2177. doi:10.1139/X05-159

Kasischke ES, Turetsky MR (2006) Recent changes in the fire regime across the North American boreal region – Spatial and temporal patterns of burning across Canada and Alaska. *Geophysical Research Letters* **33**, L09703. doi:10.1029/2006GL025677

Kasischke ES, French NHF, Bourgeau-Chavez LL, Christensen NL, Jr (1995) Estimating release of carbon from 1990 and 1991 forest fires in Alaska. *Journal of Geophysical Research* **100**, 2941–2951. doi:10.1029/94JD02957

Kasischke ES, O'Neill KP, French NHF, Bourgeau-Chavez LL (2000) Controls on patterns of biomass burning in Alaskan boreal forests. In 'Fire, Climate Change, and Carbon Cycling in the North American Boreal Forest'. (Eds E Kasischke, B Stocks) pp. 173–196. (Springer-Verlag: New York)

Kasischke ES, Hyer E, Novelli P, Bruhwiler L, French NHF, Sukhinin AI, Hewson JH, Stocks BJ (2005) Influences of boreal fire emissions on Northern Hemisphere atmospheric carbon and carbon monoxide. *Global Biogeochemical Cycles* **19**, GB1012. doi:10.1029/2004GB002300

Kasischke ES, Turetsky MR, Ottmar RD, French NHF, Hoy EE, Kane ES (2008) Evaluation of the composite burn index for assessing fire severity in Alaskan black spruce forests. *International Journal of Wildland Fire* **17**, 515–526. doi:10.1071/WF08002

Key CH, Benson NC (2006) FIREMON Landscape Assessment (LA): Sampling and Analysis Methods. USDA Forest Service, Rocky Mountain Research Station, General Technical Report, RMRS-GTR-164-CD. (Fort Collins, CO)

Kokaly R, Rockwell B, Haire S, King T (2007) Characterization of post-fire surface cover, soils, and burn severity at the Cerro Grande Fire, New Mexico, using hyperspectral and multispectral remote sensing. *Remote Sensing of Environment* **106**, 305–325. doi:10.1016/J.RSE.2006.08.006

NASA Goddard Space Flight Center (2008) 'Landsat 7 Science Data Users Handbook.' (Landsat Project Science Office: Greenbelt, MD) Available at http://landsathandbook.gsfc.nasa.gov/handbook/handbook_toc.html [Verified 2008]

Lentile LB, Holden ZA, Smith AMS, Falkowski MJ, Hudak AT, Morgan P, Lewis SA, Gessler PE, Benson NC (2006) Remote sensing techniques to assess active fire characteristics and post-fire effects. *International Journal of Wildland Fire* **15**, 319–345. doi:10.1071/WF05097

Michalek JL, French NHF, Kasischke ES, Johnson RD, Colwell JE (2000) Using Landsat TM data to estimate carbon release from burned biomass in an Alaskan spruce forest complex. *International Journal of Remote Sensing* **21**, 323–338. doi:10.1080/014311600210858

Miller JD, Thode AE (2007) Quantifying burn severity in a heterogeneous landscape with a relative version of the delta Normalized Burn Ratio (dNBR). *Remote Sensing of Environment* **109**, 66–80. doi:10.1016/J.RSE.2006.12.006

Patterson MW, Yool SR (1998) Mapping fire-induced vegetation mortality using Landsat Thematic Mapper data: A comparison of linear transform techniques. *Remote Sensing of Environment* **65**, 132–142. doi:10.1016/S0034-4257(98)00018-2

Qi J, Chehbouni A, Huete AR, Kerr YH, Sorooshian S (1994) A Modified Soil Adjusted Vegetation Index. *Remote Sensing of Environment* **48**, 119–126. doi:10.1016/0034-4257(94)90134-1

Rogan J, Franklin J, Roberts DA (2002) A comparison of methods for monitoring multitemporal vegetation change using Thematic Mapper imagery. *Remote Sensing of Environment* **80**, 143–156. doi:10.1016/S0034-4257(01)00296-6

Roy DP, Boschetti L, Trigg SN (2006) Remote sensing of fire severity: Assessing the performance of the normalized burn ratio. *IEEE Geoscience and Remote Sensing Letters* **3**, 112–116. doi:10.1109/LGRS.2005.858485

Skinner WR, Shabar A, Flannigan MD, Logan K (2006) Large forest fires in Canada and the relationship to global sea surface temperatures. *Journal of Geophysical Research* **111**, D14106. doi:10.1029/2005JD006738

Smith AMS, Wooster MJ, Drake NA, Dipotso FM, Falkowski MJ, Hudak AT (2005) Testing the potential of multi-spectral remote sensing for retrospectively estimating fire severity in African Savannahs. *Remote Sensing of Environment* **97**, 92–115. doi:10.1016/J.RSE.2005.04.014

Soja AJ, Cofer RW, Shugart HH, Sukhinin AI, Stackhouse PWJ, McRae DJ, Conard SG (2004) Estimating fire emissions and disparities in boreal Siberia (1998–2002). *Journal of Geophysical Research* **109**, D14S06. doi:10.1029/2004JD004570

Trigg S, Flasse S (2001) An evaluation of different bi-spectral spaces for discriminating burned shrub-savannah. *International Journal of Remote Sensing* **22**, 2641–2647. doi:10.1080/01431160110053185

van der Werf G, Randerson JT, Giglio L, Collatz G, Kasibhatla P, Arellano A (2006) Interannual variability of global biomass burning emissions from 1997 to 2004. *Atmospheric Chemistry and Physics* **6**, 3423–3441.

van Wagtendonk JW, Root R, Key CH (2004) Comparison of AVIRIS and Landsat ETM+ detection capabilities for burn severity. *Remote Sensing of Environment* **92**, 397–408. doi:10.1016/J.RSE.2003.12.015

Verbyla DL, Kasischke ES, Hoy EE (2008) Seasonal and topographic effects on estimating fire severity from Landsat TM/ETM+ data. *International Journal of Wildland Fire* **17**, 527–534. doi:10.1071/WF08038

Zhu Z, Key C, Ohlen D, Benson N (2006) Evaluate Sensitivities of Burn-Severity Mapping Algorithms for Different Ecosystems and Fire Histories in the United States. Department of Interior Final Report to the Joint Fire Science Program, JFSP 01-1-4-12. (Sioux Falls, SD)

Manuscript received 20 June 2008, accepted 26 June 2008